Accelerated nuclear quantum effects sampling with open path integrals

Guglielmo Mazzola[a)]
Theoretische Physik, ETH Zurich, 8093 Zurich, Switzerland
Matthias Troyer
Theoretische Physik, ETH Zurich, 8093 Zurich, Switzerland and
Quantum Architectures and Computation Group, Microsoft Research, Redmond, WA 98052, USA

(Dated: 4 August 2016)

We numericaly demonstrate that, in double well models, the autocorrelation time of open path integral Monte Carlo simulations can be much smaller compared to standard ones using ring polymers. We also provide an intuitive explanation based on the role of *instantons* as transition states of the path integral pseudodynamics. Therefore we propose that, in all cases when the ground state approximation to the finite temperature partition function holds, open path integral simulations can be used to accelerate the sampling in realistic simulations aimed to explore nuclear quantum effects.

arXiv:1608.01262v1 [physics.comp-ph] 29 Jul 2016

I. INTRODUCTION

Nuclear quantum effects (NQE) are of utmost importance in a broad class of compounds containing light atoms. For example, due to the pivotal role of the hydrogen bond, the zero point motion of the protons strongly affects the description of water and related aqueous system even at room temperature[1–4]. Moreover, under particular conditions, such as high pressure[5] or adsorption on surfaces[6], also proton tunneling events[7] occur frequently and change the physics of the systems. NQE are also essential for describing, even at the qualitative level, the phase diagram of high pressure hydrogen, the simplest condensed matter system[8–12]. Here, the tiny free energy differences between competing crystal structures, computed with the classical nuclei approximations, implies that the inclusion of NQE reorders the energetically favourable lattices at any given pressure. The most important consequence concerns the long sought low-temperature metallization of dense hydrogen[13–15] which, in the solid phase, crucially depends on the lattice structure. NQE are also important in the dense liquid phase up to temperatures of 2000 K, as they may explain residual differences between numerical simulations[11,16,17] and experiments[18] concerning the molecular dissociation and metallization in the fluid phase.

Path integral Monte Carlo (PIMC) and path integral molecular dynamic (PIMD) simulations are the most popular approach in realistic simulations to reproduce NQE as far as equilibrium properties are concerned. These methods directly arise from the Feynman path integral formulation of quantum mechanics and are able to simulate exactly the quantum statistic when the distinguishable particles approximation holds, as in the above condensed matter systems examples.

To briefly introduce this technique we start from the expression for the partition function Z:

$$Z = \int dx \langle x|e^{-\beta H}|x\rangle \tag{1}$$

where x is the quantum particle coordinate (the generalization to arbitrary dimensions is straightforward), $\beta = 1/k_B T$ is the inverse temperature and H is the Hamiltonian of the system. We first notice that the operator $e^{-\beta H}$ corresponds to an evolution in imaginary time β. We employ the Trotter-Suzuki approximation, which is based on the possibility to neglect to commutator between the non-commuting terms of $H = T + V$ (with $[T, V] \neq 0$), if the imaginary propagation time, τ, is small, i.e. $e^{-\tau(T+V)} \approx e^{-\tau T} e^{-\tau V}$. In typical condensed matter Hamiltonians, $T = 1/2m\ \partial^2/\partial x^2$ is the kinetic operator, and $V(x)$ is the potential energy, which can either be given by a empirical force fields or by *ab-initio* calculations, such as quantum Monte Carlo or density functional theory. Splitting the imaginary time evolution into P small time steps of length $\delta_\tau = \beta/P$, the path integral expression for Eq. (1) then becomes

$$Z \propto \int dx_1 dx_2 \cdots dx_P \exp \sum_{i=1}^{P} S_i \ , \tag{2}$$

where $S_i = K_i + U_i$ is the *action* of each step. $K_i = (x_{i-1} - x_i)^2/(2\delta_\tau/m)$ is the kinetic part and $U_i = \delta_\tau/2(V(x_{i-1} - x_i)$, in the so-called *primitive* approximation. Notice that $x_1 = x_P$ (closed boundary conditions in imaginary time), for evaluating the trace of the density operator.

This provides an analogy between a quantum system and a classical system with an additional dimension: Eq. (2) is a classical configurational integral and the multidimensional object $(x_1, \cdots, x_{P-1}) \equiv \mathbf{x}(\tau)$ can be viewed as a *ring-polymer*, whose elements are connected by springs. Each element is labeled by its position along the imaginary time axis, with $0 \leq \tau < \beta$. We refer to the Ref. 19 for a detailed review of path-integrals. An essential feature of Eq. (2) is that the integrand is always positive, and hence the distribution $\exp \sum_{i=1}^{P} S_i$ can be

a)gmazzola@phys.ethz.ch

sampled by means of Metropolis Monte Carlo methods or Molecular Dynamics (MD) simulations.

We note that now the computational effort is increased by at least a factor P compared to the classical nuclei approximation. For this reason several techniques have been proposed to boost the efficiency of this approach, such as colored-noise thermostats[20,21], ring-polymer contraction approaches[22,23] and multiple time-step MD[24]. Here we propose a simple approach, which can be combined with the above-mentioned techniques and can be straightforwardly applied to any existing software package for path integral simulations. Our technique is based on simulations with open boundary conditions in imaginary time. It is applicable in the low temperature limit, when the thermal quantum density distribution can be safely approximated by the ground state one.

Notice that the idea of using open path integrals in the realm of realistic simulations is certainly not new. Indeed open paths have been employed to find the ground state – this method was originally called *path integral ground state*[25–27](PIGS) — or to compute off-diagonal operators, such as the momentum, in helium[28–31] or liquid water[32]. To this end they have also been used to study NQE in water in the pioneering work of Morrone and Car[2]. This technique is also connected with the *reptation* Monte Carlo[33,34] technique, which employs a different update scheme for the open path. The main result of our paper is that open paths could also greatly reduce autcorrelation times in path integral based simulations and thus lead to more efficient simulations

II. INSTANTONS IN THE PIMC PSEUDODYNAMICS

Connections between exact quantum dynamics and PIMD approaches, such as Centroid Molecular Dynamics[35] and Ring Polymer Molecular Dynamics[36] have been discussed for a while[37–39], and have recently gained attention in the completely different field of adiabatic quantum optimization. There, PIMC is employed to simulate and predict the behaviour of quantum annealing devices[40–42] which use quantum tunneling to solve combinatorial optimization problems[43,44].

In particular, in Ref. 45, tunneling events in a ferromagnetic ising model have been studied with PIMC. This spin system can ne described by an effective double well model and it has been numerically demonstrated that PIMC tunneling events occurs with a rate k which scales exactly, to leading exponential order, with the gap squared, Δ^2, of the system, i.e. of the tunneling splitting energy squared.

Moreover it has been also shown that, if path integrals with open boundary conditions (OBC) in imaginary time are employed, the tunneling rate scales simply with Δ, thus providing a quadratic speed-up over the standard PIMC approach. The simple picture that has been provided in Refs. 45 and 46 to understand this scaling lies into the *instanton* theory of tunneling. Below we summarize t.he results of these papers.

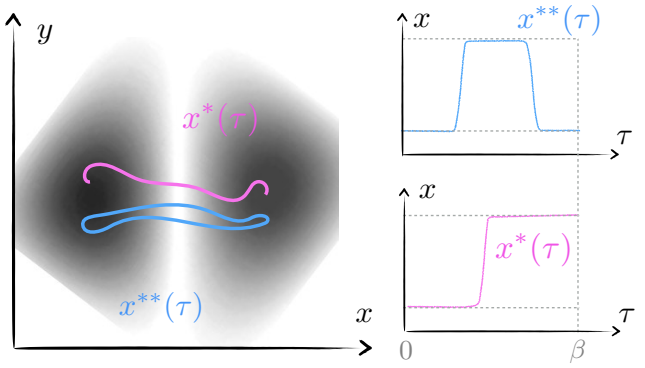

FIG. 1. (color online). *Left.* Cartoon of the typical instantonic paths in configuration space, with PBC, $\mathbf{x}^{**}(\tau)$ (cyan) and OBC in imaginary time, $\mathbf{x}^{*}(\tau)$ (pink). These paths are transition states of the PIMC and PIGS pseudodynamics respectively (in the space of imaginary time trajectories) in double well models (sketched in the grey scale heatmap). *Right.* Instantonic trajectories (projected ont ethe reaction cooordinate x axis) as a function of the imaginary time τ. Notice that PIMC instantons have to cross twice the barrier to fulfill the PBC constrain.

Let us start with the PIMC (or equivalently PIMD) simulation, where we samples paths $\mathbf{x}(\tau, t)$ at each update along the simulation time axis t, and these paths are distributed according the functional $S(\mathbf{x}(\tau))$ as in Eq. (2). We notice that, if the underlying pseudodynamics used to sample the paths is given by a first order Langevin dynamics, $\partial\mathbf{x}(\tau,t)/\partial t = -\delta S/\delta\mathbf{x}(\tau,t) + \eta(\tau,t)$ this analogy between quantum statistic and classical statistical mechanics have been already worked out in the *stochastic quantization* approach by Parisi and Wu[47] in the context of Quantum Field Theory. Here, the velocity of the (deformations of) path $\partial\mathbf{x}(\tau,t)/\partial t$, are linked to the generalized forces $\delta S/\delta\mathbf{x}(\tau,t)$ and a gaussian white noise $\eta(\tau,t)$ satisfying the obvious fluctuation-dissipation relation. If the system displays bi-stable minima, then the transition state of the pseudodynamics is given by the point $\mathbf{x}_{TS}(\tau)$ satisfying $\delta S(\mathbf{x}_{TS}(\tau))/\delta\mathbf{x}(\tau) = 0$ and which is not already in one of the attraction basins corresponding to the two minima[47–50].

Finding this transition state is generally very complicated, but in the case of a double well potential $V(x)$ this can be done analytically. Here, the dominant contribution to the integral comes from the stationary action path $\mathbf{x}^{**}(\tau)$ (determined exactly by the condition $\delta S(\mathbf{x}(\tau))/\delta\mathbf{x}(\tau) = 0$) which is called instanton[51–53]. This trajectory in imaginary time corresponds to a particle moving in the inverted potential $-V(x)$ (see Fig. 1) and it is possible to evaluate the action S at this point.

Following Ref. 45 the amplitude is given by

$$\exp(-S[\mathbf{x}^*(\tau)]) \propto \Delta \quad (\textit{instanton}), \tag{3}$$

where $\mathbf{x}^*(\tau)$ is the open trajectory which connects the

two classical turning points under the barrier, near the minima, and Δ is the *tunneling* splitting. Notice that, when computing the (diagonal) density matrix $\rho(x)$ periodic boundary conditions (PBC) in imaginary time are required. Now the integral over the *closed* paths it is dominated by the imaginary time trajectory $\mathbf{x}^{**}(\tau)$ that moves under the barrier starting, reaches the turning point, and returns. Therefore the saddle point extimation of the integral gives a *squared* tunneling amplitude

$$\exp(-S[\mathbf{x}^{**}(\tau)]) \propto \Delta^2 \quad (\textit{double instanton}), \qquad (4)$$

due to the cost of creating an instanton and an anti-instanton (see Fig. 1). Coming back to the PIMC pseudodynamics, according to Kramers theory[54], the escape rate is $k \propto e^{-S(\mathbf{x}_{TS})}$, and therefore $k \propto \Delta^2$ if standard closed path integrals are used, whereas $k \propto \Delta$ if the paths are opened. In the following, in short, we will address the first approach as simply PBC, while the latter as OBC.

In this paper we extend the study of Ref. 45 from spin hamiltonians to continuous variables models, which are relevant for realistic quantum simulations. We demonstrate that the same quadratic speedup, in sampling tunneling events, occurs in a double well model, in which we can tune separately the width and the height of the energy barrier. We also show that it is possible to sample from ground state distribution $|\psi_0(x)|^2$ by considering the center of the open-path $\mathbf{x}^*(\tau = \beta/2)$, whereas the tails $\mathbf{x}^*(\tau = 0)$, $\mathbf{x}^*(\tau = \beta)$ sample from the ground state distribution $\psi_0(x)$. Moreover, in the armonic case it is also possible to sample from correct finite temperature distribution $\rho_\beta(x)$ by using the center of the path.

In the following we provide some prototypical examples to demonstrate this feature.

III. DOUBLE WELL POTENTIAL

Let us consider the following one-dimensional double well potential,

$$V(x) = \begin{cases} \lambda(x - x_0)^4 - (x - x_0)^2, & x \geq x_0 \\ 0, & -x_0 \leq x \leq x_0 \\ \lambda(x + x_0)^4 - (x + x_0)^2, & x \leq -x_0 \end{cases} \qquad (5)$$

with $\lambda, x_0 > 0$. We can separately tune the width and the height of the barrier, varying λ and x_0. The energy barrier is $\Delta V = 1/4\lambda$, and the distance between the two minima is $d = 2(x_0 + \sqrt{1/2\lambda})$ (see inset of Fig. 2) Decreasing λ reduces the energy splitting Δ, as the two wells become deeper and more separated. The parameter x_0 only increases the well separation but doesn't change the potential energy barrier.

Following Ref. 45 we measure the mean first tunneling time (MFTT), defined as the number of MC updates required to find the system in the right well, if the particle is localized in the left one at the beginning of the simulation. From Fig. 2 we see that the MFTT scales as $1/\Delta^2$

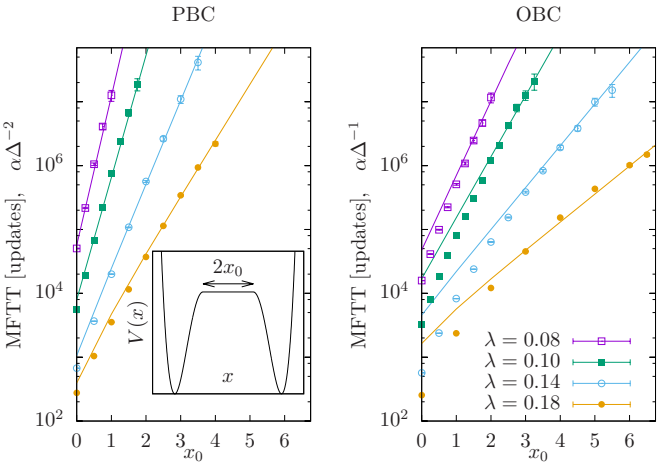

FIG. 2. (color online). Average MFTT tunneling time with PIMC (for PBC and OBC) as a function of x_0 for different values of λ, at $\beta = 20$, corresponding to a temperature always much lower than the barrier height. The inset shows the shape of double well potential $V(x)$, which barrier width (at top) is $2x_0$. Notice that for OBC, the measured MFTT is smaller than the one predicted by the $1/\Delta$ formula, when the tunneling rate is large. This happens because both the $\mathbf{x}^*(\tau)$ and the $\mathbf{x}^{**}(\tau)$ channel contribute to the tunneling.

when PBC are used, whereas it scales as $1/\Delta$ for OBC, as the parameters x_0 and λ change. The exact gap value are obtained using a discrete variable representation (DVR) technique[55]. This scaling relation holds for PIMC with local Metropolis updates and PIMD with first and second order Langevin thermostats. As far as standard PIMC is concerned, this means that the scaling of tunneling rate in a double well model $k \propto \Delta^2$ is correctly reproduced[56]. Therefore, we expect equilibrium PIMC or PIMD simulations to faithfully describe tunneling rate ratios as a function of the various control parameters, such as density, isotope masses and the accuracy of the potential energy surface $V(x)$ which can be obtained by different electronic techinques[4,57–60].

We find that for sufficiently low temperatures, it is possible to sample from the correct ground state distribution $|\psi_0(x)|^2$ by considering the center of the open-path $\mathbf{x}^*(\tau = \beta/2)$, whereas the tails $\mathbf{x}^*(\tau = 0)$, $\mathbf{x}^*(\tau = \beta)$ sample from the ground state distribution $\psi_0(x)$. Notice that, in the PIGS[25] approach this would be the mixed distribution $\psi_0(x)\psi_T(x)$, but in this case the trial wavefunction is $\psi_T(x) = 1$. In Fig. 3 we see that it is possible to sample from the exact equilibrium distribution $\rho(x) \approx |\psi_0|^2$ while having a considerable speed-up in the sampling, using OBC and considering the replicas located in the center of the path.

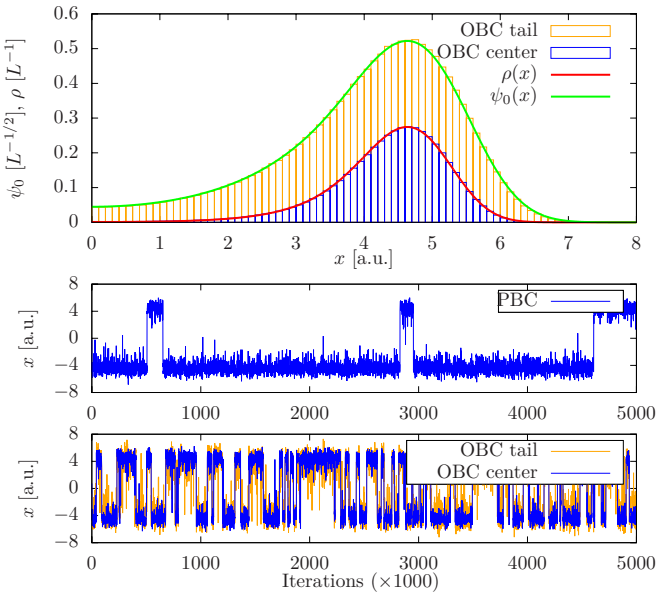

FIG. 3. (color online). Top panel: position distributions (histograms) obtained considering the center (blue) or the tail (orange) of the OBC path. The distributions are area-normalized respectively with the exact $\rho(x) \approx |\psi_0|^2$ distribution (red) and the exact ground state $\psi_0(x)$ (green). We plot only for $x > 0$ and we use $x_0 = 3$ and $\lambda = 0.14$ in Eq. (5). The difference between the sampled distrubutions and the reference ones are negligible. We perform simulations at low temperatures, $\beta = 20 \gg \Delta V$. Middle and lower panel: the position of the particle as the simulation progresses for PBC and OBC (both for center and tail). As expected the tunneling rate is much larger for OBC.

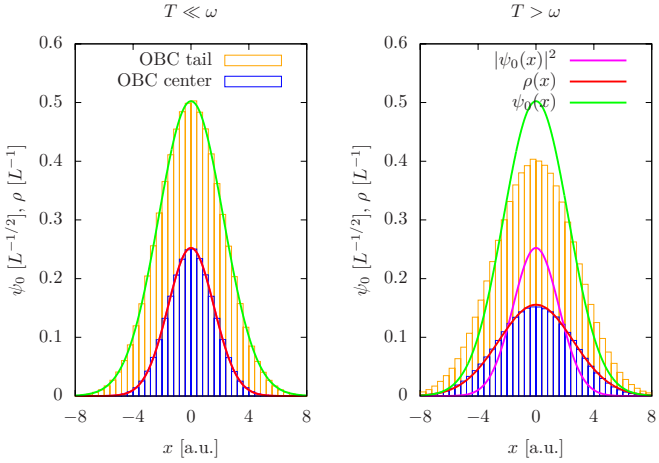

FIG. 4. (color online). Position distribution for harmonic potential at two different temperatures. We sample the distribution at the center (blue) and at the tails (orange) of the open path. At low temperature (left panel) the distributions coincide respectively with the exact $|\psi_0|^2$ (magenta) and $|\psi_0|$ (green) ones. Interestingly the center of the path still sample the correct finite temperature distribution $\rho(x)$ (red) at larger temperature $T > \omega$.

IV. HARMONIC OSCILLATOR AND FINITE TEMPERATURE SIMULATIONS

We next investigate the ability of OBC to simulate finite temperature properties. We consider a harmonic potential of the form $V(x) = 1/2\ m\omega^2 x^2$, with $m = 1/2$ and $\omega = 0.4$. We perform simulations at temperatures respectively smaller and larger than energy gap ω. From Fig. 4 we see that the center of the OBC path still samples the exact thermal distribution $\rho(x)$, which differs from the simple ground state density $\psi_0(x)^2$ at large temperature. Unfortunately this property does not hold in the general case, for example, in the double well model considered above, we make an error of $\approx 10\%$ in the sampled distribution, at a large temperatures $T \sim \Delta V$. Indeed, in this case, the trade-off between accuracy and speed-up has to be carefully checked for non-zero temperature simulations.

V. CONCLUSIONS

We have studied the autocorrelation properties of path integral based equilibrium simulations with periodic and open boundary conditions in imaginary time. While the former technique is widely used to simulate nuclear quantum effects at finite temperature, the latter is also a well established approach — although less popular compared to its PBC counterpart — used to calculate ground state properties.

We have numerically demonstrated that the autocorrelation time of open paths simulations can be much smaller than the corresponding periodic case. In a double well model, characterized by quantum tunneling mechanism, we obtain a clear quadratic speedup as a function of the tunneling energy splitting Δ, which in turn is given by the shape of the potential energy barrier. This holds in both continuos space and spin models. We also provide an intuitive explanation based on the role of *instantons* in the PIMC pseudodynamics.

Therefore we propose that, in all cases when the ground state approximation to the finite temperature partition function holds, open path integral simulations should be used and will accelerate the sampling. The computational gain of using open paths is clearly system dependent, but is expected to be particularly large when rare quantum tunneling events become important.

VI. ACKNOWLEDGEMENTS

This work was supported by the European Research Council through ERC Advanced Grant SIMCOFE by the Swiss National Science Foundation through NCCR QSIT, and by Microsoft Research. This paper is based upon work supported in part by ODNI, IARPA via MIT Lincoln Laboratory Air Force Contract No. FA8721-05-C-0002. The views and conclusions contained herein are

those of the authors and should not be interpreted as necessarily representing the official policies or endorsements, either expressed or implied, of ODNI, IARPA, or the U.S. Government. The U.S. Government is authorized to reproduce and distribute reprints for Governmental purpose not-withstanding any copyright annotation thereon. We acknowledges useful discussions with P. Faccioli and S.Sorella. MT acknowledges hospitality of the Aspen Center for Physics, supported by NSF grant PHY-1066293.

[1] M. Ceriotti, W. Fang, P. G. Kusalik, R. H. McKenzie, A. Michaelides, M. A. Morales, and T. E. Markland, Chemical reviews (2016).
[2] J. A. Morrone and R. Car, Phys. Rev. Lett. **101**, 017801 (2008).
[3] M. Ceriotti and D. E. Manolopoulos, Physical review letters **109**, 100604 (2012).
[4] M. Ceriotti, J. Cuny, M. Parrinello, and D. E. Manolopoulos, Proceedings of the National Academy of Sciences **110**, 15591 (2013).
[5] M. Benoit, D. Marx, and M. Parrinello, Nature **392**, 258 (1998).
[6] X. Meng, J. Guo, J. Peng, J. Chen, Z. Wang, J.-R. Shi, X.-Z. Li, E.-G. Wang, and Y. Jiang, Nature Physics **11**, 235 (2015).
[7] J. O. Richardson, C. Pérez, S. Lobsiger, A. A. Reid, B. Temelso, G. C. Shields, Z. Kisiel, D. J. Wales, B. H. Pate, and S. C. Althorpe, Science **351**, 1310 (2016).
[8] S. A. Bonev, E. Schwegler, T. Ogitsu, and G. Galli, Nature **431**, 669 (2004).
[9] C. J. Pickard and R. J. Needs, Nature Physics **3**, 473 (2007).
[10] V. Labet, R. Hoffmann, and N. W. Ashcroft, The Journal of Chemical Physics **136**, 074504 (2012).
[11] M. A. Morales, J. M. McMahon, C. Pierleoni, and D. M. Ceperley, Physical Review Letters **110**, 065702 (2013).
[12] G. Mazzola, S. Yunoki, and S. Sorella, Nature Communications **5**, 3487 (2014).
[13] M. I. Eremets and I. A. Troyan, Nature Materials **10**, 927 (2011).
[14] R. T. Howie, C. L. Guillaume, T. Scheler, A. F. Goncharov, and E. Gregoryanz, Phys. Rev. Lett. **108**, 125501 (2012).
[15] P. Dalladay-Simpson, R. T. Howie, and E. Gregoryanz, Nature **529**, 63 (2016).
[16] G. Mazzola and S. Sorella, Physical Review Letters **114**, 105701 (2015).
[17] S. Sorella and G. Mazzola, arXiv preprint arXiv:1605.08423 (2016).
[18] M. Knudson, M. Desjarlais, A. Becker, R. Lemke, K. Cochrane, M. Savage, D. Bliss, T. Mattsson, and R. Redmer, Science **348**, 1455 (2015).
[19] D. M. Ceperley, Rev. Mod. Phys. **67**, 279 (1995).
[20] M. Ceriotti, G. Bussi, and M. Parrinello, Physical Review Letters **103**, 030603 (2009).
[21] M. Ceriotti, M. Parrinello, T. Markland, and D. Manolopoulos, Journal of Chemical Physics **133**, 124104 (2010).
[22] T. E. Markland and D. E. Manolopoulos, The Journal of chemical physics **129**, 024105 (2008).
[23] C. John, T. Spura, S. Habershon, and T. D. Kühne, Phys. Rev. E **93**, 043305 (2016).
[24] V. Kapil, J. VandeVondele, and M. Ceriotti, The Journal of chemical physics **144**, 054111 (2016).
[25] A. Sarsa, K. E. Schmidt, and W. R. Magro, J. Chem. Phys. **113**, 1366 (2000).
[26] S. Constable, M. Schmidt, C. Ing, T. Zeng, and P.-N. Roy, The Journal of Physical Chemistry A **117**, 7461 (2013), PMID: 23738885.
[27] S. Pilati and M. Troyer, Physical review letters **108**, 155301 (2012).
[28] D. Ceperley and E. Pollock, Can. J. Physics **65**, 1416 (1987).
[29] G. Bertaina, M. Motta, M. Rossi, E. Vitali, and D. Galli, Physical review letters **116**, 135302 (2016).
[30] A. Roggero, F. Pederiva, and G. Orlandini, Physical Review B **88**, 094302 (2013).
[31] J. E. Cuervo, P.-N. Roy, and M. Boninsegni, The Journal of chemical physics **122**, 114504 (2005).
[32] J. A. Morrone, V. Srinivasan, D. Sebastiani, and R. Car, The Journal of Chemical Physics **126** (2007).
[33] S. Baroni and S. Moroni, Phys. Rev. Lett. **82**, 4745 (1999).
[34] G. Carleo, F. Becca, S. Moroni, and S. Baroni, Physical Review E **82**, 046710 (2010).
[35] J. Cao and G. A. Voth, The Journal of Chemical Physics **99** (1993).
[36] I. R. Craig and D. E. Manolopoulos, The Journal of Chemical Physics **121** (2004).
[37] S. Jang, A. V. Sinitskiy, and G. A. Voth, The Journal of Chemical Physics **140** (2014).
[38] B. J. Braams and D. E. Manolopoulos, The Journal of Chemical Physics **125** (2006).
[39] T. J. H. Hele, M. J. Willatt, A. Muolo, and S. C. Althorpe, The Journal of Chemical Physics **142** (2015).
[40] E. Farhi, J. Goldstone, S. Gutmann, and M. Sipser, arXiv preprint quant-ph/0001106 (2000).
[41] E. Farhi, J. Goldstone, S. Gutmann, J. Lapan, A. Lundgren, and D. Preda, Science **292**, 472 (2001).
[42] M. Johnson, M. Amin, S. Gildert, T. Lanting, F. Hamze, N. Dickson, R. Harris, A. Berkley, J. Johansson, P. Bunyk, et al., Nature **473**, 194 (2011).
[43] S. Boixo, T. F. Ronnow, S. V. Isakov, Z. Wang, D. Wecker, D. A. Lidar, J. M. Martinis, and M. Troyer, Nature Physics **10**, 218 (2014).
[44] T. F. Rønnow, Z. Wang, J. Job, S. Boixo, S. V. Isakov, D. Wecker, J. M. Martinis, D. A. Lidar, and M. Troyer, Science **345**, 420 (2014).
[45] S. V. Isakov, G. Mazzola, V. N. Smelyanskiy, Z. Jiang, S. Boixo, H. Neven, and M. Troyer, arXiv preprint arXiv:1510.08057 (2015).
[46] Z. Jiang, V. N. Smelyanskiy, S. V. Isakov, S. Boixo, G. Mazzola, M. Troyer, and H. Neven, arXiv preprint arXiv:1603.01293 (2016).
[47] G. Parisi, Y.-s. Wu, et al., Scientia Sinica **24**, 483 (1981).
[48] M. Sega, P. Faccioli, F. Pederiva, G. Garberoglio, and H. Orland, Physical review letters **99**, 118102 (2007).
[49] E. Autieri, P. Faccioli, M. Sega, F. Pederiva, and H. Orland, The Journal of chemical physics **130**, 064106 (2009).
[50] G. Mazzola, S. a Beccara, P. Faccioli, and H. Orland, The Journal of chemical physics **134**, 164109 (2011).
[51] S. Coleman, Phys. Rev. D **15**, 2929 (1977).
[52] H. Forkel, ArXiv High Energy Physics - Phenomenology e-prints (2000).
[53] E. M. Chudnovsky and J. Tejada, *Macroscopic Quantum Tunneling of the Magnetic Moment*, Cambridge, UK: Cambridge University Press, 1998.
[54] P. Hänggi, P. Talkner, and M. Borkovec, Reviews of modern physics **62**, 251 (1990).
[55] D. T. Colbert and W. H. Miller, The Journal of chemical physics **96**, 1982 (1992).
[56] U. Weiss, H. Grabert, P. Hänggi, and P. Riseborough, Physical Review B **35**, 9535 (1987).
[57] K. Laasonen, M. Sprik, M. Parrinello, and R. Car, The Journal of Chemical Physics **99**, 9080 (1993).
[58] A. Zen, Y. Luo, G. Mazzola, L. Guidoni, and S. Sorella, The Journal of chemical physics **142**, 144111 (2015).
[59] M. Del Ben, M. Schönherr, J. Hutter, and J. VandeVondele, The Journal of Physical Chemistry Letters **4**, 3753 (2013).
[60] T. D. Kühne, M. Krack, and M. Parrinello, Journal of Chemical Theory and Computation **5**, 235 (2009).